

Effect of Heat Treatment on Structural and Electronic Transition of Nano-Crystalline Titanium Dioxide Film

Haidar Gazy Lazim AL-Sabah¹, Khalid. I. Ajeel² and Aseel Hassan³

¹(Misan University, College of Basic Education, Department of Science, Iraq)

²(Basrah University, College of Education for pure science, Department of Physics, Iraq)

³(Sheffield Hallam University, Materials and Engineering Research Institute, Sheffield, UK)

Abstract: Nanocrystalline of titanium dioxide nano films were deposited by spin coating method on silicon and ITO-glass substrates at 2000 rpm, in which starting material of Titanium Isopropoxide ($C_{12}H_{28}O_4Ti$). X-ray diffraction (XRD) patterns confirmed that polycrystalline TiO_2 anatase phase formation. The intensity of XRD peaks increases with the increase in heat treatment and better crystallinity takes place at higher temperature. The morphology of deposited films were characterized by atomic force microscope (AFM); with increasing heat treatment, both the particle size and surface roughness increased. The particle size value were 2.184, 2.374, 4.834, 5.125, and 8.336 nm and RMS roughness values were 0.161, 0.223, 0.552, 0.810 and 1.494 nm for films deposited at 250, 350, 450, 550 and 650 °C respectively. Optical properties measurements (Transmittance, T , and Absorptance, A) of (TiO_2) films showed high transparency. It is observed that maximum transmittance at 250 °C for wavelength range 320-900 nm. The optical band gap of the films has been found to be in the range 3.28-3.62 eV for the forbidden direct electronic transition and 3.45-3.75 eV for the allowed direct transition for the different heat treatment.

Keywords - Nanoanatase TiO_2 , Sol-Gel, XRD, AFM, Transmittance, Absorptance

I. INTRODUCTION

Titanium dioxide (TiO_2) has attracted considerable attention for its potential applications in optical components including solar cell, photocatalysis, chemical sensors, and optical filters [1-5]. The material can be formulated as thin films by using a variety of techniques such as pulsed laser deposition (PLD) [6-8], chemical vapour deposition [9,10], and sol-gel coating [11,12]. TiO_2 has three main crystal phases (anatase, rutile, and brookite). Among these phases, anatase phase, which is a meta-stable phase, is also chemically and optically active and suitable for photocatalyst [13]. In dye-sensitized solar cells, photo-electrodes prepared using anatase phase TiO_2 gives better solar cell efficiency compared to the other crystal structures. Optical properties of TiO_2 include a wide band gap, high transparency in the visible spectrum and a high refractive index over a wide spectral range (from ultraviolet (UV) to the far infrared (IR)). Nanocrystalline titania (TiO_2) is also a promising semiconductor for applications based on its photoconductivity. The reported optical gap of TiO_2 is in the range of 3-3.7 eV corresponding to the ultraviolet region of the solar spectrum [14].

In the present study, we report on the synthesis and characterization of nanocrystalline TiO_2 and influences of heat treatment on structural and electronic transition of nanocrystalline titanium dioxide films prepared by sol-gel spin coating. One of the most important techniques is spectroscopic ellipsometry, which has been found favourably for non-destructive, characterization of thin solid films and bulk materials, especially semiconductors. This technique is of high sensitivity, high accuracy, of being able to easily in situ measure both optical constant and thickness simultaneously [15]. The effect of heat treatment temperatures on the particle size of the nanoanatase TiO_2 film was investigated. We found that particle size could be controlled by the heat treatment temperatures in pure nanoanatase thin films.

II. EXPERIMENTAL

Nanocrystalline like structured TiO_2 films have been prepared by sol-gel spin coating method using a standard photoresist spinner (Model 4000 Electronic Micro System). The gel was spin coated on Si and a cleaned ITO-glass substrates at 2000 rpm for nano films of (TiO_2) prepared from Titanium Isopropoxide (TIP) of chemical construction ($C_{12}H_{28}O_4Ti$) of purity (99.99%), also from (Acetic Acid) (CH_3COOH) of purity (99.5%), and also from (Ethanol) (C_2H_5OH) with purity of (99.7%). These materials were prepared of (Aldrich Chemicals Company). These films have been characterized by XRD, and Spectroscopic ellipsometry were investigated on TiO_2 films spin coated onto silicon substrates using a Woolam M-2000V that rotated compensator spectroscopic ellipsometry in the wavelength of range from 370-1000 nm. The fixed degree of the angle of incidence was 70°. The thickness of the TiO_2 film was found to be approximately 70 nm. The surface morphology was examined by atomic force microscopy (AFM-Digital Instruments Nano Scope). The optical absorptance and transmittance measurements were made on TiO_2 nano films by UV-Vis spectrophotometer at a normal incident

of light in the wavelength range of 320-900 nm. After coating, the sol-coated glass substrate was immediately placed in a preheated oven. A furnace type, (CAUTION) was used in this work which has a temperature range of (25-1000 °C).

III. RESULT AND DISCUSSION

X-ray diffraction patterns of the TiO₂ nano films have been shown in Fig. 1 to Fig. 5 for different heat treatment temperature 250, 350, 450, 550, and 650 °C. It is obvious that the film is polycrystalline.

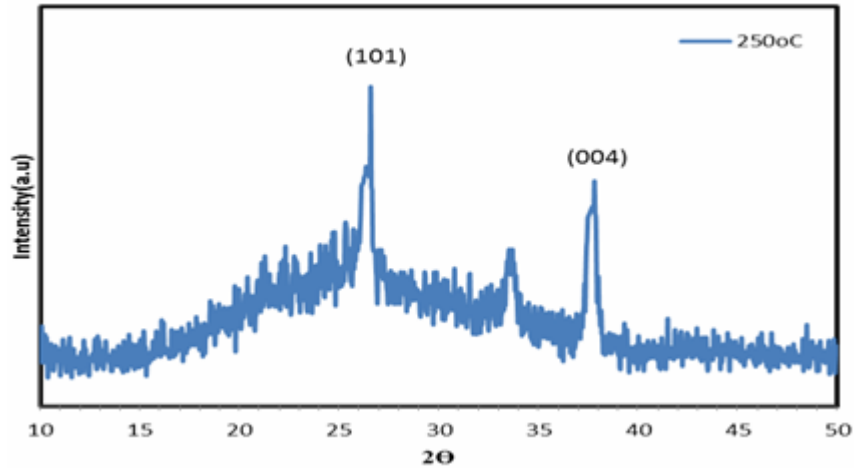


Fig.1: XRD patterns of TiO₂ films grown on ITO- glass substrates at heat treatment temperature 250°C.

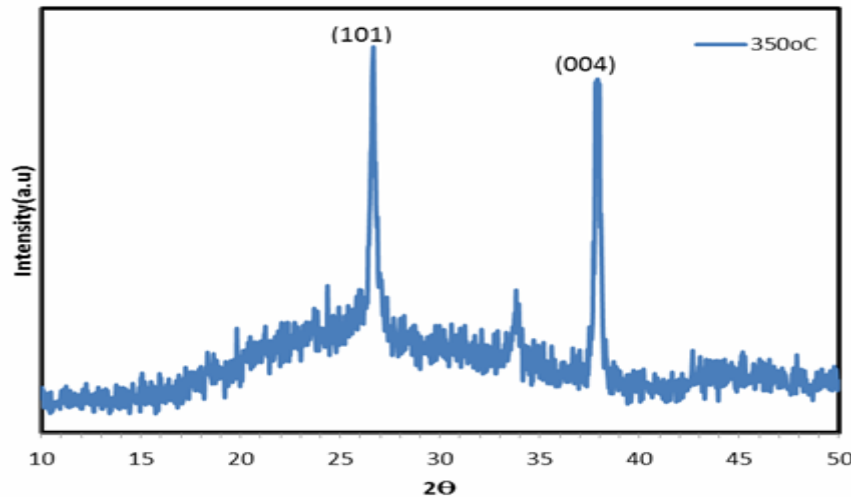


Fig. 2: XRD patterns of TiO₂ films grown on ITO- glass substrates at heat treatment temperature 350°C.

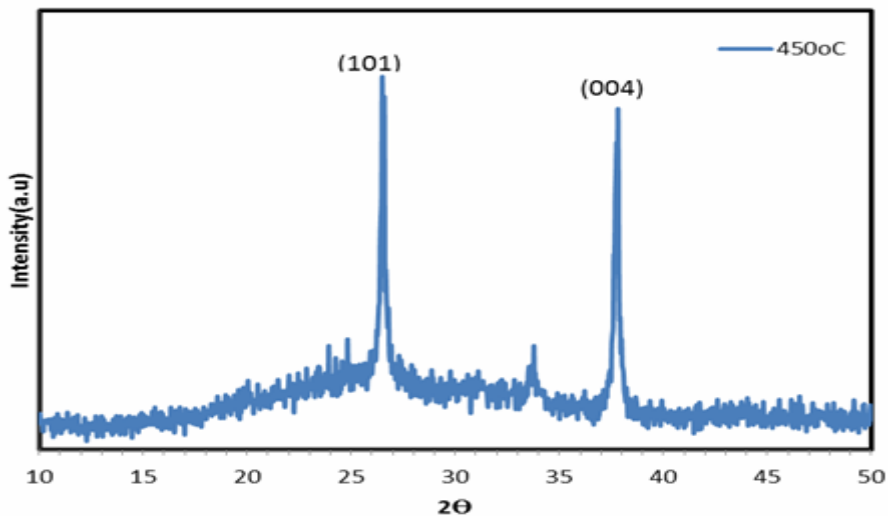


Fig. 3: XRD patterns of TiO₂ films grown on ITO- glass substrates at heat treatment temperature 450°C.

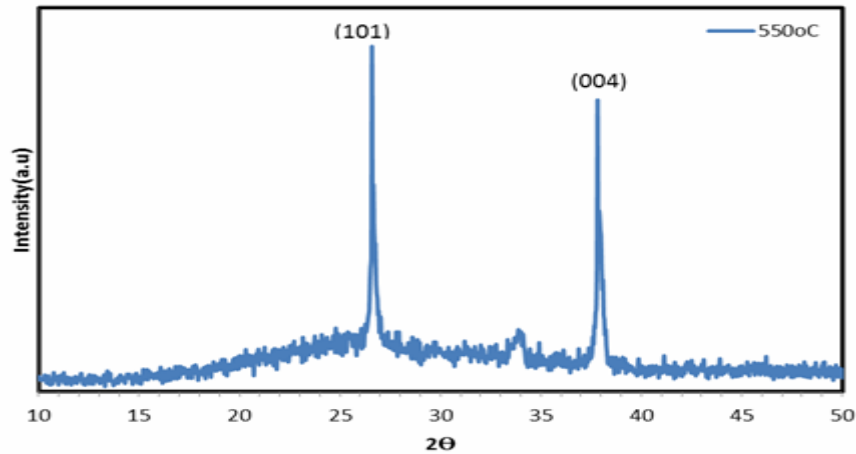


Fig. 4: XRD patterns of TiO₂ films grown on ITO- glass substrates at heat treatment temperature 550°C.

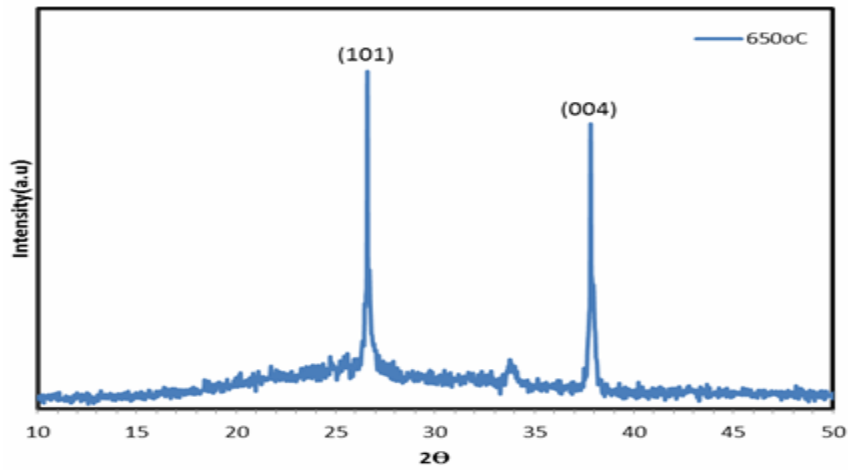


Fig. 5: XRD patterns of TiO₂ films grown on ITO- glass substrates at heat treatment temperature 650°C.

The structure of TiO₂ in XRD investigation is anatase titanium dioxide, which agrees with (ASTM data 01-071-1166) card. The intensity of XRD peaks increases as the heat treatment temperature increased and better crystallinity takes place at higher temperature (650 °C). Also the rutile and brookite forms of TiO₂ have not been observed during the investigation. The average crystallite size D_{101} of films was found to be 31.9 - 43.7 nm and the average crystallite size D_{004} of films was found to be 26.9 - 38.6 nm from the angular line width β at half maximum intensity and the diffracted angle Θ employing Scherrer relation [16-17]:

$$D_{hkl} = \frac{094\lambda}{\beta \cos \theta} \quad (1)$$

where $\lambda=0.154$ nm is the wavelength of incident x-ray. The observed XRD data peaks along with interplanar distance, d , and Miller indices (hkl) are summarized in Table 1. Average values of the lattice parameters a and c are determined from the following relation which estimated to be 3.6 and 9.5 Å° respectively from substitution of interplanar distances in Table 1 into equation:

$$\frac{1}{d^2} = \frac{h^2 + k^2}{a^2} + \frac{\ell^2}{c^2} \quad (2)$$

It can be seen that the values are very close to the standard values of 3.7 and 9.5 Å° [18].

Fig. 6 to Fig. 10 show AFM images of the pure nanoanataseTiO₂ films heated at different temperatures

Table 1: XRD data for the nanoanataseTiO₂ films.

Temperature °C	Angle (2θ) degree	Angle (2θ) degree	d values (Å)	d values (Å)	Miller indices (hkl)	FWHM degree	D _{hkl} nm
	Observed	Standard	Observed	Standard			
250	26.3736	25.308	3.3794	3.5162	(101)	0.2670	31.9
	37.5734	37.791	2.3758	2.3786	(004)	0.3247	26.9
350	26.6382	25.308	3.3464	3.5162	(101)	0.2620	32.5
	37.9201	37.791	2.3778	2.3786	(004)	0.1948	45.0
450	26.5160	25.308	3.3616	3.5162	(101)	0.2373	35.9
	37.7422	37.791	2.3758	2.3786	(004)	0.1948	45.0
550	26.9355	25.308	3.3101	3.5162	(101)	0.2273	37.5
	38.1133	37.791	2.3758	2.3786	(004)	0.2598	33.7
650	26.8474	25.308	3.3208	3.5162	(101)	0.1948	43.7
	38.0997	37.791	2.3745	2.3786	(004)	0.2273	38.6

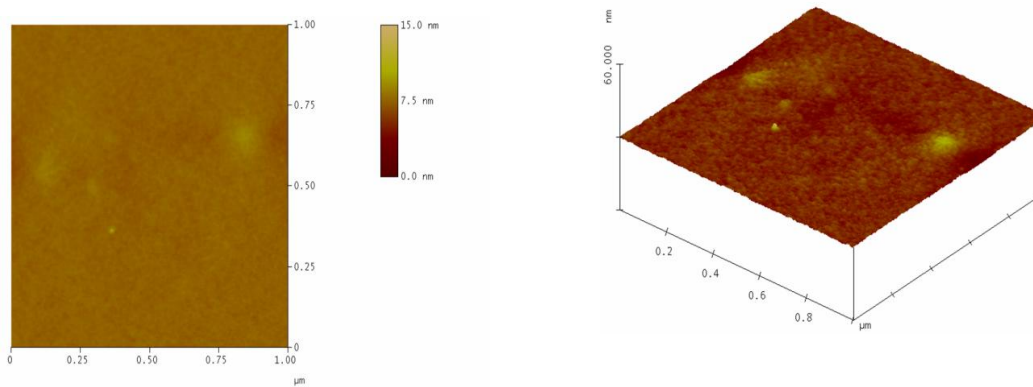


Fig. 6: Two and three-dimensional AFM images of TiO₂ films at heat treatment temperature 250°C.

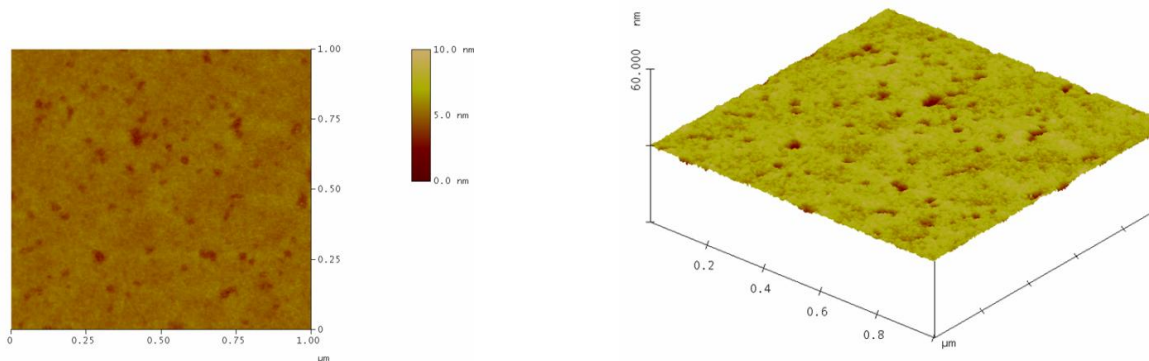


Fig. 7: Two and three-dimensional AFM images of TiO₂ films at heat treatment temperature 350°C.

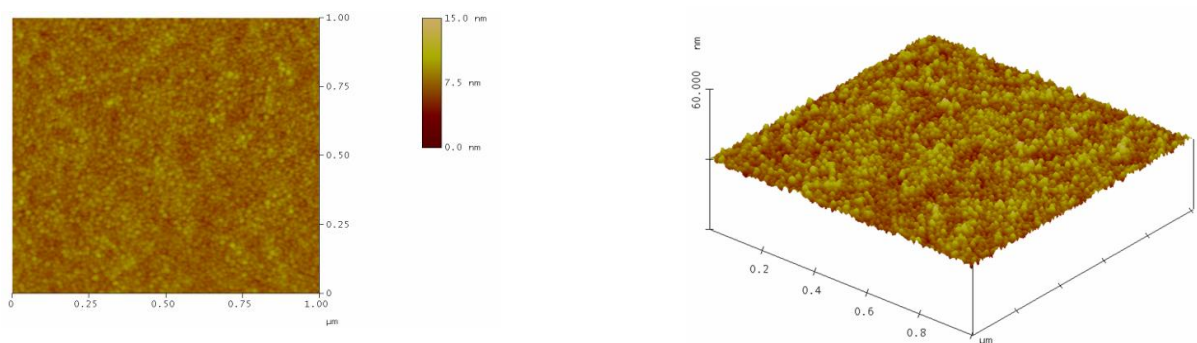


Fig. 8: Two and three-dimensional AFM images of TiO₂ films at heat treatment temperature 450°C.

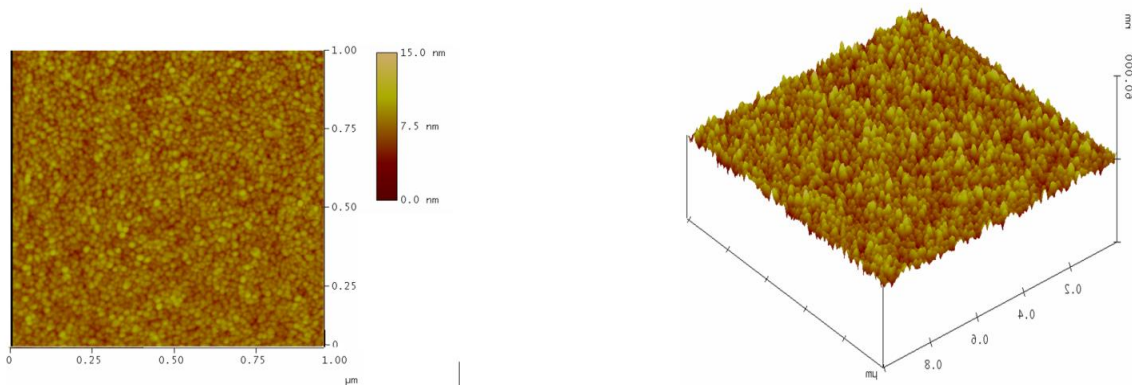


Fig. 9: Two and three-dimensional AFM images of TiO₂ films at heat treatment temperature 550°C.

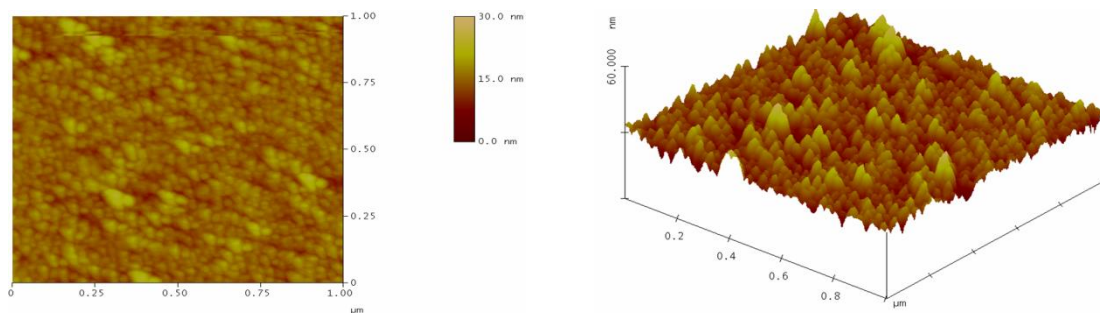


Fig. 10: Two and three-dimensional AFM images of TiO₂ films at heat treatment temperature 650°C

We observed that the particle size increased with the increasing heat treatment temperature, which was supported by the XRD results. The RMS surface roughness of the nanoanatase TiO₂ films was determined to be (0.161, 0.223, 0.552, 0.810 and 1.494 nm) and the particles size are found to be (2.184, 2.378, 4.534, 5.125 and 8.336 nm) for the 250, 350, 450, 550 and 650 °C heat treatment temperature values respectively. The results were summarized at Table 2.

Absorption spectra of pure nanoanatase TiO₂ films were analysed using a UV-Vis spectrophotometer, as shown in Fig. 11.

Table 2: AFM data for the nanoanatase TiO₂ films.

Temperature (° C)	RMS (nm)	Particle size (nm)
250	0.161	2.184
350	0.223	2.378
450	0.552	4.534
550	0.810	5.125
650	1.494	8.336

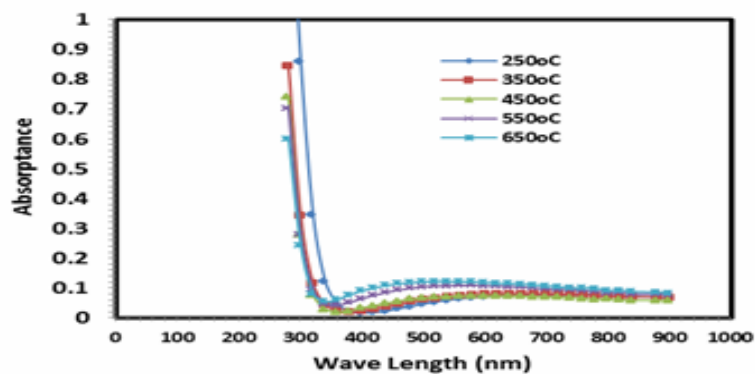


Fig. 11: Absorption spectra of TiO₂ films with different heat treatment heat treatment.

When the heat treatment temperature of the films increased, the absorption is also increased. The transmission value of the film was also investigated in the wavelength range of 320-900 nm, as shown in Fig. 12 using the UV-Vis spectrophotometer.

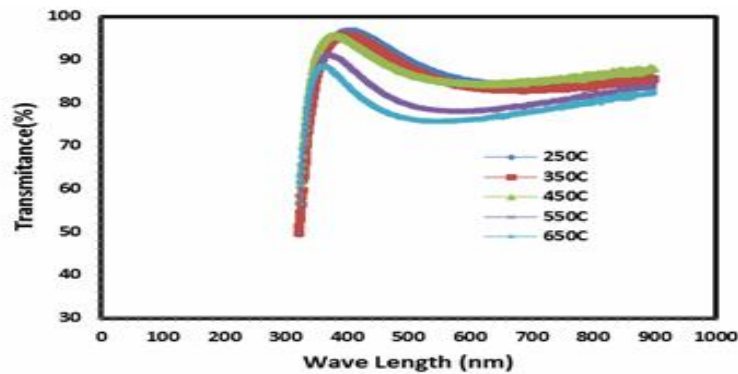


Fig. 12: Transmission spectra of TiO₂ films with different heat treatment heat treatment. It can be seen that the transmittance of the film decreased when the heat treatment temperature of the nanoanatase TiO₂ film was increased.

The band gap energy calculated by Spectrophotometric data using following equation [19].

$$\alpha h\nu = B(h\nu - E_g)^n \tag{3}$$

where α is the absorption coefficient, $h\nu$ is the photon energy in eV, E_g is the band gap energy in eV, B is constant depended on type of material, $n=1/2$ for the allowed direct transition and $n=3/2$ for the forbidden direct transition.

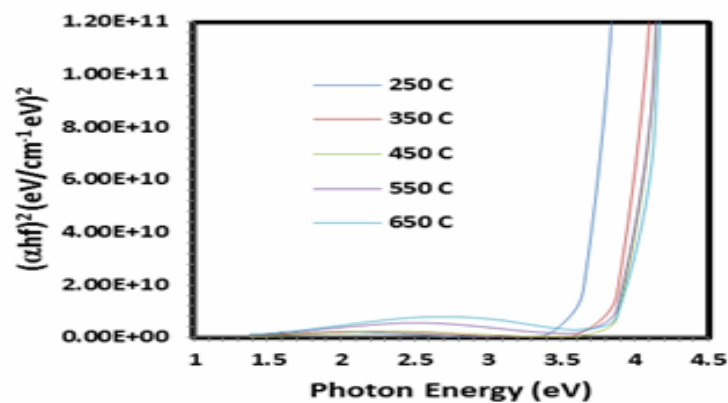


Fig. 13: $(\alpha h\nu)^2 - h\nu$ graphs of nanoanatase TiO₂ films for different heat treatment temperature.

The relations are drawn between $(\alpha h\nu)^2$, $(\alpha h\nu)^{2/3}$ and photon energy $h\nu$, as shown in Fig. 13 which illustrates allowed direct electronic transition and Fig. 14 illustrates the forbidden direct electronic transition.

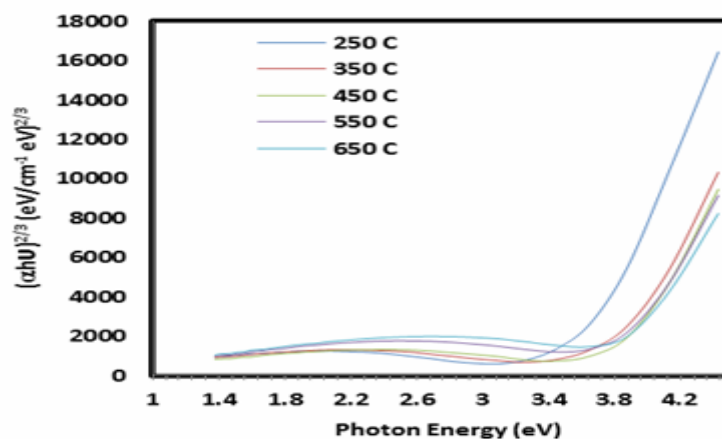


Fig. 14: $(\alpha h\nu)^{2/3} - h\nu$ graphs of nanoanatase TiO₂ films for different heat treatment temperature

The obtained band gap values are given in Table 3. This result is in good agreement with earlier studies in which a direct optical transition was reported in the range 3.3-3.79 eV [20].

Table 3: direct energy gap for allowed and forbidden direct transition for nanoanataseTiO₂ films.

Temperature (° C)	Allowed direct transition E _g (A) (eV)	Forbidden direct transition E _g (F) (eV)
250	3.45	3.28
350	3.62	3.39
450	3.68	3.6
550	3.69	3.61
650	3.75	3.62

The band gap energy of TiO₂ films changed with different particle size, as seen in the AFM results ,Table 2 , shown in Fig. 15. We observed that the particle size of pure nanoanataseTiO₂ films increased with increasing band gap energy.

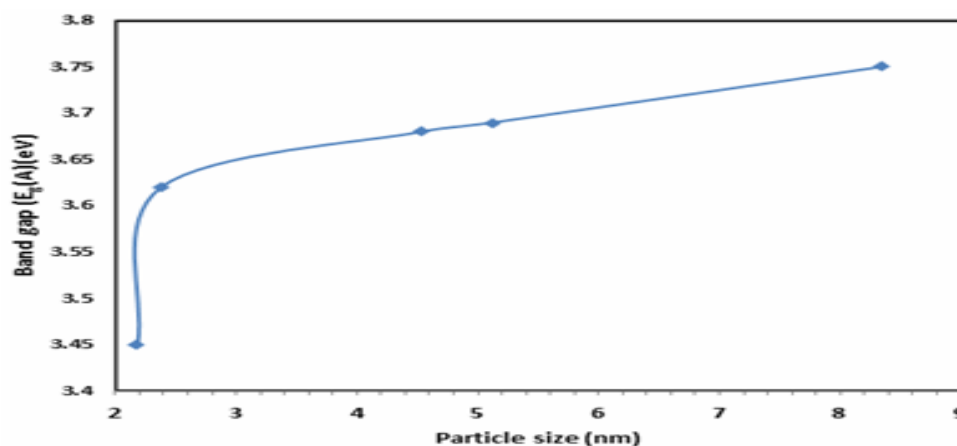


Fig. 15: Band gap energy-particle size graphs of nanoanataseTiO₂ films for different heat treatment temperature.

IV. CONCLUSION

From the present study, it can be withdrawn the following conclusions, Titanium dioxide films were prepared through a sol-gel process. The intensity of XRD peaks increases with the increase in heat treatment and better crystallinity takes place at higher temperature. The investigation of (XRD) indicates that the (TiO₂) film is polycrystalline type of (anatase). It was found that the particle size controlled by the heat treatment temperature. The results indicate that an increase in the heat treatment temperature led to the increase in the particle size of TiO₂ films because of the increasing crystallization. The roughness of pure nanoanatase TiO₂ films increased with increasing particle size. The optical absorptance of nanoanatase TiO₂ film increased with increased heat treatment temperature, while the transmittance values of the nanoanatase TiO₂ film decreased with increased heat treatment temperature. The optical band gap of the films has been found to be in the range 3.28-3.62 eV for the forbidden direct electronic transition and 3.45-3.75 eV for the allowed direct transition for the different heat treatment.

REFERENCES

- [1]. S. Sharma, M. Vishwas, K. Rao and S. Mohan, Structural and optical investigations of TiO₂ films deposited on transparent substrates by sol-gel technique, Journal of Alloys and Compounds, 471 , 2009, 244–247.
- [2]. F. Gamez, A. Reyes, P. Hurtado, E. Guille, J. A. Anta, and B. Martez, Nanoparticle TiO₂ Films Prepared by Pulsed Laser Deposition: Laser Desorption and Cationization of Model Adsorbents, J. Phys. Chem. C , 114, 2010, 17409–17415.
- [3]. C. Ayieko¹, R. Musembi¹, S. Waita¹, B. Aduda¹ and P. Jain, Structural and Optical Characterization of Nitrogen-doped TiO₂ Thin Films Deposited by Spray Pyrolysis on Fluorine Doped Tin Oxide (FTO) Coated Glass Slides, International Journal of Energy Engineering , 2(3), 2012, 67-72.
- [4]. M. Mohammadi, N. Shahtahmaseb, M. Karimipour¹, and R. Sarhadd, Characterization of nanostructured Nd-doped TiO₂ thin film synthesized by spray pyrolysis method: Structural, optical and magneto-optical properties, Indian Journal of Science and Technology, 5 (6) 2012, 2912-2916.
- [5]. C. Ayieko, R. Musembi, S. Waita, and P. Jain, Structural and Optical Characterization of Nitrogen-doped TiO₂ Thin Films Deposited by Spray Pyrolysis on Fluorine Doped Tin Oxide (FTO) Coated Glass Slides, International Journal of Energy Engineering, 2(3), 2012, 67-72.
- [6]. X. Han, G. Wang, J. Jie, X. Zhu, and J. Hou, Properties of Zn_{1-x}CoxO thin films grown on silicon substrates prepared by pulsed laser deposition, Thin Solid Films, 491, 2005, 249 – 252.

- [7]. S. Hyuck , S. Yeol , B. Jun, and I. Seongil, Pulsed laser deposition of ZnO thin films for applications of light emission," *Applied Surface Science*,154, 2000, 458–461.
- [8]. A. Singh, M. Kumar, R. Mehra, A. Wakahara, and A. Yoshida, Al-doped zinc oxide (ZnO:Al) thin films by pulsed laser ablation, *J. Indian Inst.*,81, 2001, 527-533.
- [9]. R. Capan, N. Chaure, A. Hassan, Optical dispersion nanocrystalline titania thin films, *Semiconductor Science and Technology*, 19(7), 2004, 198-202.
- [10]. D. Rathee, M. Kumar, and S. Arya, Deposition of nanocrystalline thin TiO₂ films for MOS capacitors using Sol-Gel spin method with Pt and Al top electrodes, *Solid State Electronics*, 76, 2012, 71-76.
- [11]. N. Ibrahim E. Yusrianto and Z. Ibrahim , Effect of Different TiO₂ Preparation Techniques on the Performance of the Dielectric Bolometer as a Distance Sensor , *Sains Malaysiana* 41(8) ,2012, 1092-2035.
- [12]. H. Shih and R. Vasant, Sol–gel TiO₂ in self-organization process: growth, ripening and sintering, *RSC Advances*, 2(3), 2012, 2294–2301.
- [13]. M. Landmann, E. Rauls and W. Schmidt, The electronic structure and opticalresponse of rutile, anatase and brookite TiO₂, *J. Phys.* 24(5), 2012, 1-6.
- [14]. D. ThiThanh Lea, D. Vuongb, and N. Van Duya, Preparation and characterization of solid n-TiO₂/p-NiO heterojunction electrodes for all-solid-state dye-sensitized solar cells, *Solid State Electronics* 53, 2009, 1116–1125.
- [15]. H. Jiang, Q. Wei, Q. Xiyao, Spectroscopicellipsometry characterization of TiO₂ thin films prepared by the sol-gel method, *Ceramics International*, 34, 2008, 1039-1042.
- [16]. E. Lee, J. Hong, H. Kang and J. Jang, Synthesis of TiO₂ nanorod-decorated graphene sheets and their highly efficient photocatalytic activities under visible-light irradiation, *Jornal of Hazardous Materials* 219(220), 2012, 13– 18.
- [17]. I. Ganesh, A. Gupta, P. Kumar, P. Chandra , K. Radha, G. Padmanabham, and G. Sundararajan, Preparation and characterization of Co-doped TiO₂ materials for solar lightinduced current and photocatalytic applications, *Materials Chemistry and Physics* 135(4), 2012, 220-234.
- [18]. ASTM data (01-071-1166) card.
- [19]. A. P. Singh, S. Kumari, and R. Shrivastav, Iron doped nanostructured TiO₂ for photoelectrochemical generation of hydrogen, *International Journal of Hydrogen Energy* 33(2), 2008, 5363-5368.
- [20]. Z. Wang, U. Helmersson, and P. Kall, Optical properties of TiO₂ thin film prepared by aqueous sol-gel at low temperature, *Thin Solid Film*, 405(9), 2002, 50-54.